Materials Science & Engineering A 840 (2022) 142972

Contents lists available at ScienceDirect

Materials Science & Engineering A

journal homepage: www.elsevier.com/locate/msea

On the similitude relation for dislocation wall thickness under cyclic deformation

Farhan Ashraf, Gustavo M. Castelluccio *

School of Aerospace, Transport and Manufacturing, Cranfield University, Bedfordshire, MK43 0AL, UK

ARTICLE INFO

Keywords:
Similitude
Wall thickness
Persistent slip band
Cells

ABSTRACT

Dislocation substructures have been extensively characterized to explain the origin of strain hardening. Regions of high dislocation densities (walls) constrain the glide of mobile dislocations in regions of lower dislocation density (channels). Transmission electron microscopy (TEM) has shown that the distance in between walls is inversely proportional to flow stress, which is often referred as to the similitude principle. However, it still remains unclear whether a similitude scaling law exists for the dislocation wall thickness or wall fraction. The understanding of such a scaling law is instrumental to support substructure-based crystal plasticity, validate dislocation dynamics models, and explain substructure formation processes. Hence, this work surveys TEM images from various FCC metallic materials under cyclic deformation at various temperatures to assess the existence of the similitude principle for dislocation walls. The results demonstrate that the wall thickness does follow similitude, but the proportionality constant depends on the temperature for some structures.

1. Background

Cyclic deformation of face centered cubic (FCC) metallic materials results in substructures [1] formed by dislocation walls and channels. Depending on the crystallographic orientation, immobile dislocations form veins structures at low applied plastic strains, persistent slip bands (PSB) under single slip orientation, labyrinths due to Hirth locks, or cells when cross slip is profuse. The high dislocation density at walls makes their response virtually elastic, which induces a strong residual stress (or back stress) on mobile dislocations along the channels. Furthermore, these structures limit the mean free path of mobile dislocations, which otherwise move relatively unobstructed along channels. As a result, the mechanical response of metallic materials strongly depends on the morphology and wall fraction (f_w) which is often computed by the ratio [2],

$$f_w = \frac{w}{w+d}, \tag{1}$$

in which d corresponds to the distance in between walls and w is the wall thickness; note that w and d are distances that can be measured with TEM images and they are typically in the range between 0.1 and 10 μm. Other formulations [3–5] proposed to compute the wall fraction can often be approximated by Equation (1) along with a scaling factor.

Multiple constitutive models [4,6,7] have relied on the quantification of wall fractions to predict strain hardening. Recently, Castelluccio and McDowell [8] generalized these approaches for cyclic loading with a crystal plasticity model that parameterized the morphology of dislocation structures for Ni at room temperature. This model [8,74] predicts the cyclic response of crystals by introducing an intragranular back stress rate ($\dot{B}^\alpha$) that represents the constraint of sessile dislocation structures on mobile dislocations, i.,e.,

$$\dot{B}^\alpha = \frac{f_w}{1-f_w}\frac{2\mu(1-2S_{1212})}{1+4S_{1212}\mu f^S_{Hill}}\dot{\gamma}^\alpha, \tag{2}$$

where, $\dot{\gamma}^\alpha$ is the shear rate, f^S_{Hill} is the instantaneous macroscopic plastic deformation tangent, S_{1212} is the Eshelby tensor component for a prolate spheroid coordinate system [9], and μ is the shear modulus.

The intragranular back stress rate in Equation (2) is fully determined by the morphology and dimensions of dislocation structures. However, the quantification of the wall fraction for various crystal orientations, materials or temperatures is still an open question. When multiple structures coexist (e.g., PSBs surrounded by veins), the total wall fraction depends on the relative predominance of each structure and their characteristic wall fraction. Recent efforts [10] based on Equation (2) for predicting single- and poly-crystal responses for various materials

* Corresponding author.
E-mail address: castellg@cranfield.ac.uk (G.M. Castelluccio).

https://doi.org/10.1016/j.msea.2022.142972
Received 20 October 2021; Received in revised form 8 March 2022; Accepted 8 March 2022
Available online 10 March 2022
0921-5093/Crown Copyright © 2022 Published by Elsevier B.V. This is an open access article under the CC BY license (http://creativecommons.org/licenses/by/4.0/).

suggested that f_w may depend on temperature for some structures, but notably, not for all. Other efforts using dislocation dynamics modelling [11–13] have aimed to characterizing these structures, but the approaches are at their infancies due to their high computational demands.

In a series of papers, Sauzay and Kubin [14–16] extensively discussed the experimental evidence supporting dislocation substructure scaling laws under monotonic and cyclic deformation. Their work solidly demonstrated the existence of a scaling relation (also called similitude principle) [17–20], in which the flow stress (τ) is inversely proportional to the total wall spacing,

$$\tau = K \frac{\mu b}{w + d}, \tag{3}$$

where b is the Burgers vector. On the contrary, Sauzay and Kubin do not provide a definite description of the dislocation wall thickness, arguing that "PSB wall thickness appears to follow an approximate similitude" [14] based on experimental work for PSBs.

Similitude formulation based on wall dimensions are advantageous for modeling since they often have lower experimental uncertainty compared to dislocation density measurements. Moreover, the similitude coefficient under cyclic loading ($K \approx 3$) is, as a first order approximation, independent of temperature and the material, for FCC metals with low to high stacking fault energy (SFE) [14]. Hence, the discovery of scaling laws for wall fractions can be instrumental to validate dislocation dynamics simulations and to advance novel substructure- and temperature-sensitive models. We proceed with an extensive review of experimental evidence for FCC metals under cyclic loading to demonstrate the existence of scaling relations for the wall thickness and wall fractions.

2. Quantification of wall fraction for different substructures

2.1. Vein structures

Cyclic loading at very low strain amplitudes (typically below 1×10^{-4}) results in vein structures, which correspond to coplanar loops that accumulate during cycling as shown in Fig. 1 a). For well-annealed materials, the wall fraction of veins increases with the number of cycles [21,22] or the applied plastic strain [23]. Upon filling the entire volume with veins, the structure becomes unstable and transitions to other structures with lower intrinsic wall fractions. At plastic cyclic strains about 1×10^{-4} , this transition occurs during the first few thousand loading cycles [24] but it can take millions of cycles for lower applied strains [25] and it can depend on temperature [26].

Several authors [23,27] have shown that multiple FCC metals present veins with an intrinsic wall fraction independent of the temperature and occupying approximately half the total volume (i.e., equal loop patches and channels spacing). To evaluate this assessment, Fig. 1 b) presents the wall fraction computed with Equation (1) and dimensions measured in TEM images from various single crystal materials (Al, Ni, Cu, and Stainless steel) [28–34]. The error bar corresponds to the variability of measurements as demonstrated in Fig. 1 a) and depends not only on the structure variability but on the relative tilt between the glide and observation planes. The analysis results in veins fractions in the range of 0.3–0.45, which should be considered as a lower bound that could have increased upon further cycling. Hence, our analysis confirms the notion that veins can fill out up to half the volume and temperature independent.

2.2. PSB structures

Next, we compiled TEM images that depict clear ladder-type PSBs for various materials at different temperatures (Al, Ni, Cu, Ag, Au, Stainless steel) from single- and poly-crystals. The wall thickness and wall spacing were measured perpendicular to the ladder rungs as shown by Fig. 2 a). Since PSB structures result in a stress plateau [35] for plastic cyclic strain approximately between 1×10^{-4} to 1×10^{-2}, a change in plastic strain does not lead to a change in wall spacing (e.g., constant stress results in constant wall spacing in Equation (1). Hence, we compare different wall spacing by considering experiments performed temperatures from 4 K to 750 K, which results in plateaus with different stress levels (and hence different wall spacing).

Fig. 2 b) compiles the thickness and spacing measurements on TEM images from the literature. These results demonstrate that the wall thickness in PSB is consistently between $0.15 \pm 0.06 \mu m$ regardless of the temperature, applied strain, or material. Contrarily, the wall spacing is strongly sensitive to temperature and can change by a factor of ten in accordance with the similitude relation. At constant temperature, both the wall thickness and the wall spacing are approximately constant for the entire plastic strain ranges for which PSBs are stable. Hence, by combining Eqs. (1) and (2) and assuming that the wall fraction of PSBs is a function of temperature we deduce that,

$$\tau = f_w^{PSB}(T) K \frac{\mu b}{w}, \tag{4}$$

which states that PSBs wall thickness follows a scaling law with a similitude coefficient that depends on the temperature.

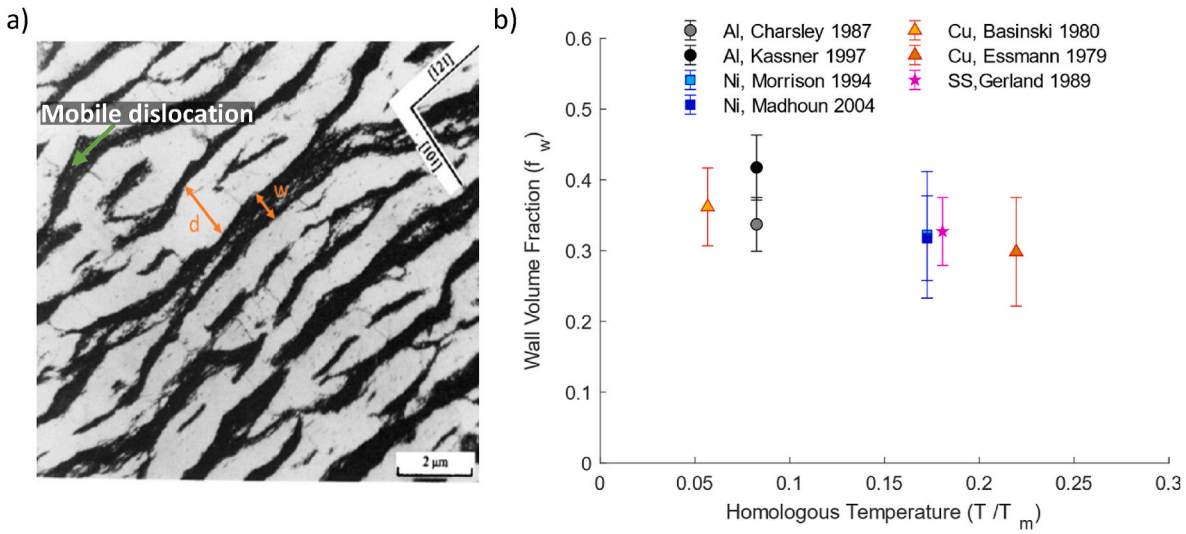

Fig. 1. a) Example of a vein structure in Cu [32] b) f_w as a function of temperature as computed from Equation (1) using TEM images from Refs. [28–34].

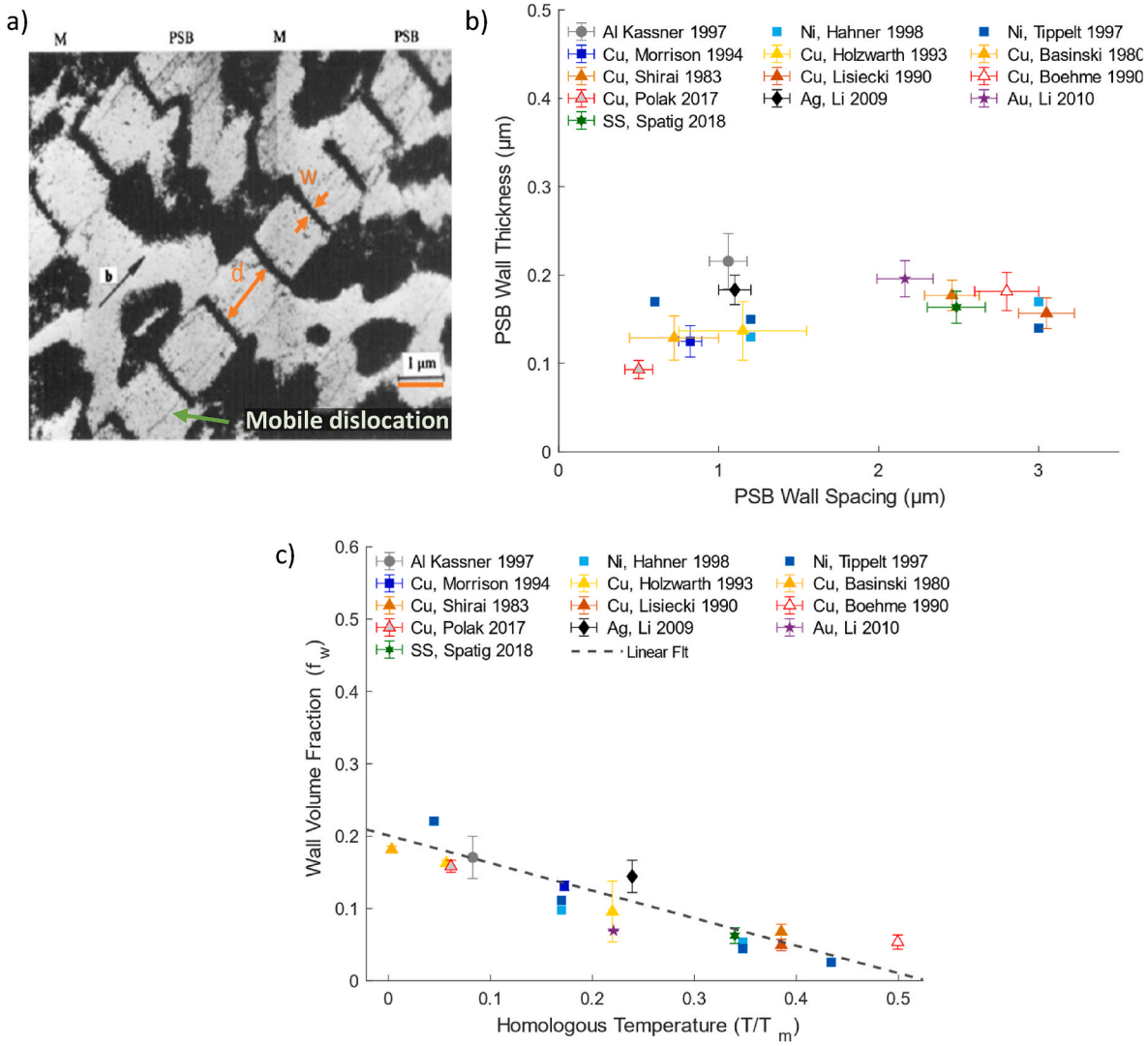

Fig. 2. a) PSB in Cu single crystal from Ref. [36] b) PSB wall thickness and wall spacing at different temperatures for different FCC metals [36–49] c) PSB wall fraction as a function of the homologous temperature. The line corresponds to the least square fitting of Equation (4).

Fig. 2 c) presents the wall fraction as a function of homologous temperature calculated with Equation (1) and Fig. 2 b). These results demonstrate that the PSB wall fraction decreases with increasing homologous temperature ($\frac{T}{T_m}$). This behavior can be parameterized as,

$$f_w = f_w^{0K} - a^* \frac{T}{T_m}, \tag{5}$$

where $f_w^{0K} = 0.21\ (\pm 0.028)$, $a = 0.38\ (\pm 0.1)$ are the coefficients and their covariance of the linear least square fitting. Note that this a robust characterization of a linear correlation fit to data from six metals and alloys at various temperatures from 4 K to 750 K.

2.3. Labyrinth structures

Following a similar procedure, we now consider TEM images of labyrinth structures (Fig. 3 a) from single- and poly-crystals to quantify the wall thickness and spacing perpendicular to the structure. Thin dislocation lines in the channels (Fig. 3b)) correspond to mobile dislocations slanted with respect to dislocation walls of the labyrinth structure. We only consider labyrinth structure for different FCC metals at plastic strain ranges of 1×10^{-3} or higher so that dislocation walls are well defined and do not have loop patches in between them. The results in Fig. 3 c) demonstrate that, similar to PSB, the wall thickness does not significantly vary for a range of materials and loading conditions. When comparted to PSBs, the average wall thickness varies between 0.07 μm to 0.15 μm, which is 30% shorter than that from PSBs. Similarly, the wall spacing in labyrinth structures cycled at room temperature is about 0.1 μm, compared to 1.2 μm for PSB.

The different scaling between PSB and labyrinth structures can be rationalized by observing the TEM work from Winter et al. [50]. Their work, reproduced in Fig. 4, presents the seamless coexistence of ladders-type PSBs and labyrinth structure in Cu. PSBs are inclined to labyrinth walls, which are aligned along the [100] and [001] directions [51]. Mobile dislocations are evident along [101] direction, making them perpendicular to the PSBs rungs, but inclined to labyrinth structures. Since the system is in static equilibrium, mobile dislocations bowing out perpendicular to the PSBs undergo comparable shear stress to those dislocations bowing out inclined to the labyrinth structures. Hence, similar bow out stresses leads to similar dislocation length, but different wall spacing due to the different relative angles between walls and mobile dislocations.

Fig. 4 makes it evident that not only the wall spacing but also the thickness is smaller in labyrinth structures as compared to PSBs for mobile dislocations under equivalent loading. The difference in spacing is a factor of $\sqrt{2}$, which corresponds to the projection of the wall spacing

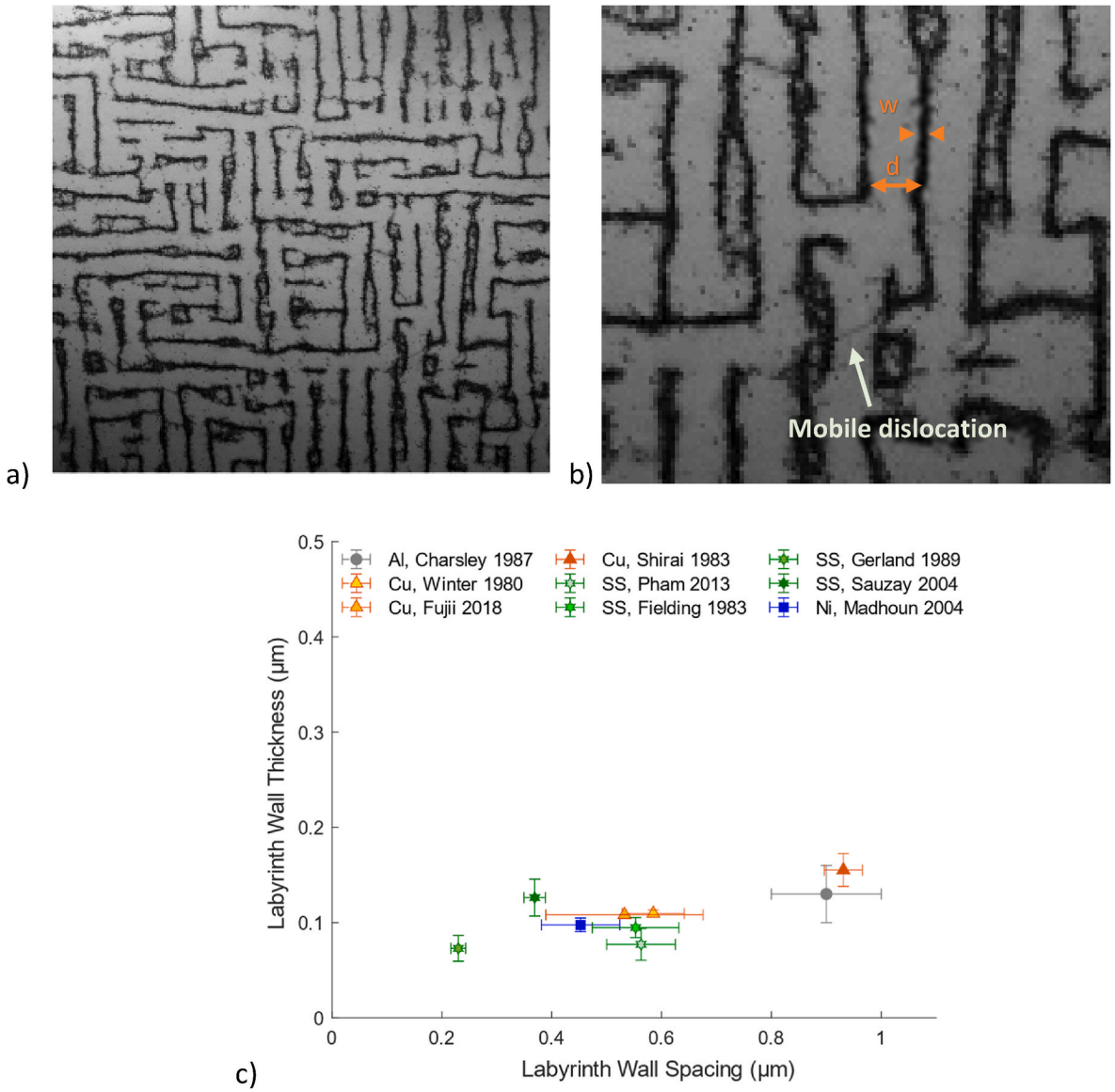

Fig. 3. a) Labyrinth structure in Cu single crystal with stress axis parallel to [001] under $\gamma_{pl} = 3.5 \times 10^{-3}$ from Ref. [52]. Note the thin screw dislocations that sit in the channels slanted with respect to the walls from Ref. [52]. b) Detail showing think lines in between walls that correspond to mobile screw dislocations. c) Relationship between wall thickness and wall spacing in labyrinth structure for different FCC metals [31,34,46,50,52–54].

along the screw direction and that agrees with our analysis from Figs. 2 and 3. The implications of this conclusion are significant because the similitude coefficient is about 30% smaller in labyrinth compared to PSBs. On the contrary, since both wall thickness and spacing are affected by the $\sqrt{2}$ factor, the wall fraction is the same for both PSBs and Labyrinth. As a result, we deduce that,

$$\tau = K\,\frac{\mu b}{\sqrt{2}d} = \frac{1}{\sqrt{2}} f_w^{PSB}(T) K\,\frac{\mu b}{w}. \tag{6}$$

Which states that labyrinth wall thickness follows the same scaling law as PSBs (which depends on temperature), but the wall spacing similitude constant differs in a factor of $\frac{1}{\sqrt{2}}$.

2.4. Cell structures

Finally, we consider TEM images that present cell structures after cyclic deformation in Al, Ni, Cu, Ag, and Stainless steel in single- and poly-crystals. Cell structures form upon profuse cross slip as a result of activation of multiple slip systems [56], which is observed in crystals oriented closely aligned for loading along [111]. Cell spacing and wall thickness were measured as shown by Fig. 5a), in which the error bar conveys the variability of coexisting cells. In contrast to PSBs, increasing the plastic strain range results in higher stresses. Hence, various cell dimensions can be measured at the same temperature but different plastic strain ranges.

Fig. 5b) presents the cell wall thickness and spacing measured from TEM images. Lower temperatures and lower strain amplitudes [31,43,57–59] results in less refined cell structure and larger error bars. Contrarily, TEM data [40,46,60,61] corresponding higher deformation temperature and higher strain amplitude showed saturated equiaxed cells shown with relatively smaller error bar in Fig. 5 b). This figure further shows that cell wall thickness has lower uncertainty as compared to cell size.

The results in Fig. 5 b) are strikingly different from those Fig. 2 b) and Fig. 3 b). The cell the wall thickness varies from 0.04 μm to 0.4 μm as a function of applied strain and temperature. At the same time, the cell diameter also changes proportionally to the wall thickness such that the cell wall fraction (f_w^{cell}) is approximately constant with values of 0.05–0.2

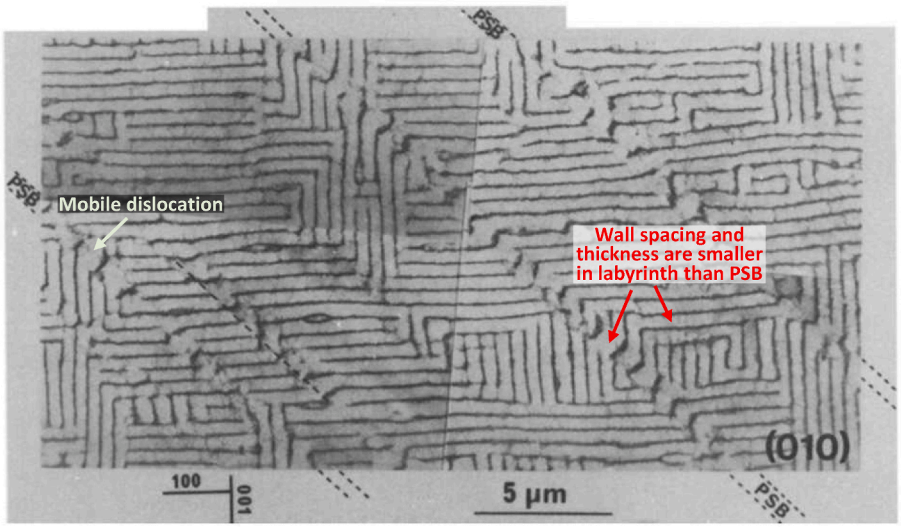

Fig. 4. Labyrinth structure in pure Cu with dislocation walls parallel to 001 traces. PSBs are visible at the bottom right with walls parallel to [110] from Ref. [55]. A similar result was found by in Ref. [50].

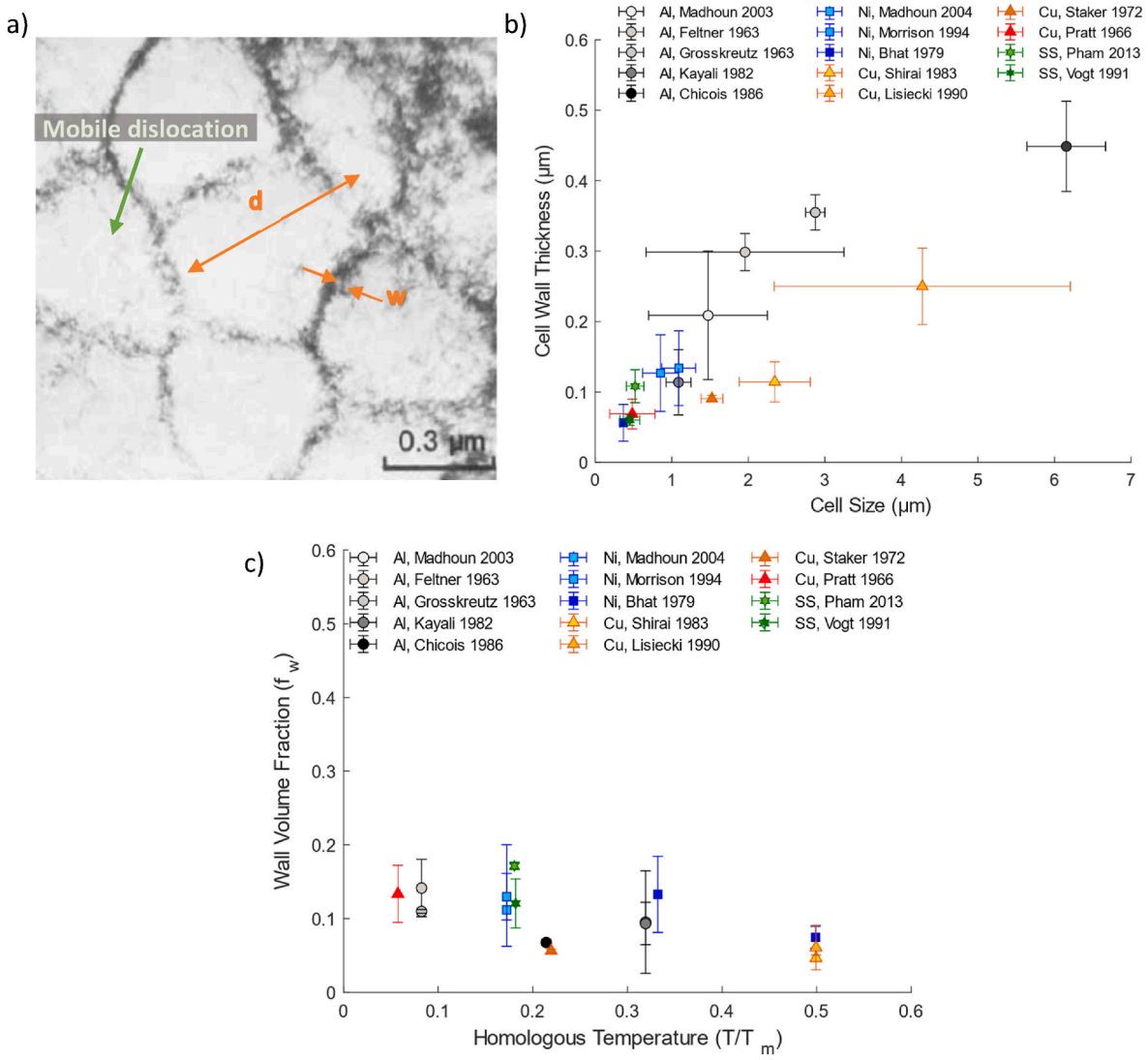

Fig. 5. a) Mobile screw dislocation gliding in a cell in Ni [60] b) Cu [30] Correlation between cell wall size and wall thickness at different temperatures and strain amplitudes for different FCC metals [30,31,42,43,46,57,58,60–64]. c) Cell wall fraction as a function of the homologous temperature.

as shown in Fig. 5c).

Prior efforts [65,66] have found that cell wall thickness varies under monotonic loading. For example, Knoesen and Kritzinger [66] characterized that the wall fraction is fairly constant with an approximate value of 0.5 for commercial Cu. These results demonstrate that cell wall thickness under cyclic and monotonic deformation is proportional to cell diameter and follow a similitude law such that,

$$\tau = K\,\frac{\mu b}{d} = f_w^{cell} K\,\frac{\mu b}{w_{cell}}, \tag{7}$$

with the understanding f_w^{cell} is temperature independent.

Equation (7) assumes that the wall spacing similitude constant K for PSBs is identical to that for cells, which is indeed suggested by Sauzay and Kubin [14]. We can further support this notion by considering the coexistence between various structures as exemplified by Fig. 6. Following a similar argument as before, cells coexist with other structures in static equilibrium with similar spacing in between walls (e.g., Fig. 6). Since mobile dislocation inside cells are approximately perpendicular to walls (e.g., Fig. 5a), no correction be required such as that for labyrinth structures. Moreover, we can consider similitude constant K for PSB as an upper, but close bound for cells similitude coefficient.

3. Discussion

The analysis of Equations (4), (6) and (7) explains the ambivalent position from Sauzay and Kubin [14] in concluding whether wall thickness follows similitude. Under isothermal experimental conditions, the wall thickness follows identical similitude for PSBs and cells, and requires a 30% correction for labyrinth structures. Such correction can be easily obscured by experimental error from mixing labyrinth with veins, tilt angle, or lack of stress saturation. Hence, it would seem evident that wall thickness follows similitude. However, upon a change of temperature only cells structures would follow a scaling law with the same similitude coefficient, which would lead to the conclusion that wall thickness does not follow a single scaling law. To make the analysis even more complex, different FCC metals at identical homologous temperatures would result in similar wall thickness and wall fraction for PSBs and labyrinth, but not for cells.

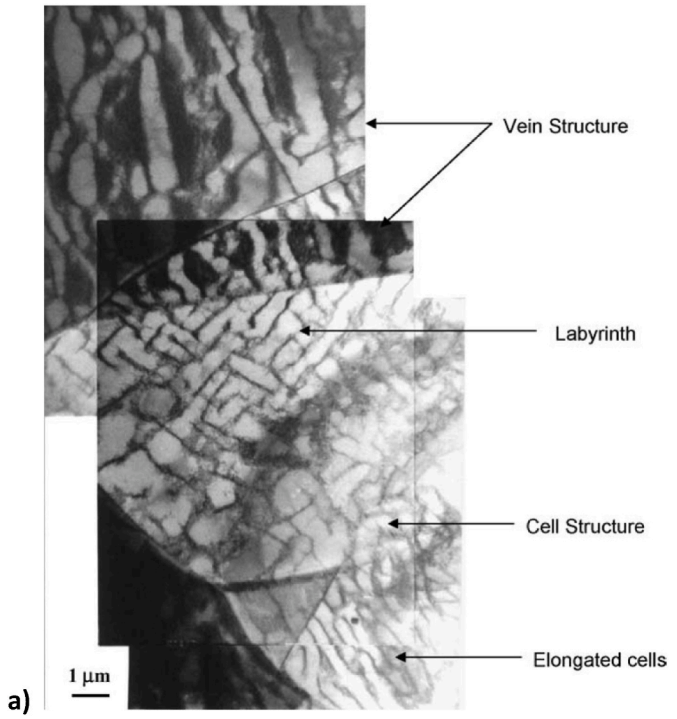

Fig. 6. Coexistence of dislocation structures in static equilibrium in polycrystalline Ni [31].

A second consideration regards to the origin of the temperature dependence (or lack of) for the wall thickness. In this sense, much research has linked refinement of cell structures with the activation of cross slip, which can enable recovery mechanisms. Hence, we hypothesize that the lack of extended cross slip in PSBs, and the formation of strong Hirth locks in labyrinth structures prevent the recovery mechanisms in walls, making their wall thickness material and temperature independent. On the contrary, cross slip enables recovery at cell walls and results on temperature dependent wall thickness.

3.1. Implications for novel modeling approaches

One major challenge in modeling plastic deformation is the identification of parameters, which are often not unique or do not describe accurately the grain scale response [67,68]. Our recent efforts have proposed physics [8,10,69] rather than mathematics strategies [70,71] for augmenting experimental data. These strategies [8,10] predict single- and poly-crystal responses by relying on mesoscale parameters informed with TEM data and the identification of the structure from slip systems activation.

In this context, scaling laws that are *material-invariant* are instrumental to relate strain hardening with the morphology of dislocation structures by means of Equations (2) and (3). We demonstrated that the characteristic wall fraction of the structures in Table 1 are not significantly sensitive to the material composition. Hence, veins and cells have relatively constant athermal wall fractions while PSBs and labyrinth wall fractions decrease with temperature. Moreover, wall fractions of PSBs and labyrinth structures are proportional.

The extensive analysis of TEM images led to novel material-invariant formulations that reduce the number of unknown parameters in Equation (2). Furthermore, they enable modelling strain hardening across temperatures assuming a single wall spacing similitude constant K for all structures along with the wall fractions in Table 1. Our results can also support the modeling of temperature-dependent size effects [72] by affecting the accommodation factor (f_{Hill}^{S}) in Equation (2) as a means to account for the finite domain of a crystal or grain relatively to the substructure length scale. Notably, Eshelby finite domain corrections can also be linked to strain gradient theories [73] to naturally convey size effects.

Finally, we highlight that our results enables the validation of modeling approaches not only from the macroscopic response, but also from the mesoscale wall morphology from TEM. In addition, dislocation dynamics modeling [11–13] have the potential to inform the morphology of structures prior to being tested. Hence, constitutive formulations that rely on the formulations in Table 1 have potential for multiscale experimental validation and hierarchical modelling.

4. Conclusions

This work surveyed extensively literature TEM images with dislocation structures resulting from cyclic loading saturation. The analysis demonstrates that the wall thickness follows similitude, albeit the relation applies exclusively to a specific dislocation structure. Under some circumstances such as constant temperature, a similar relation can apply to various structures.

Table 1
Characteristic wall fractions for various dislocation structures after cyclic deformation in FCC metals.

Veins	PSBs	Labyrinth	Cells
$f_w^{Veins} \approx 0.5$	$f_w^{PSB} \approx 0.21 - 0.38\frac{T}{T_m}$	$f_w^{Lab} \approx \sqrt{2} f_w^{PSB}$	$f_w^{Cells} \approx 0.05$ *to* 0.2

Our analysis has identified a notable difference in wall fraction evolution between structures that can or cannot cross slip. The former seems to have a constant temperature-independent wall fraction in monotonic and cyclic. On the contrary, PSBs and labyrinth have wall fractions that are temperature dependent.

This work provides the bases to predict the wall fractions of different structures based on the local stress. The formulations proposed not only support substructure sensitive crystal plasticity modelling, but they also provide clear trends to benchmark dislocation dynamics modelling. Ongoing work seeks to implement wall fraction similitude laws to predict the local anisotropic mechanical response of grains in polycrystals.

Data availability

The authors confirm that the data supporting the findings of this study are available within the article or supplementary material.

CRediT authorship contribution statement

Farhan Ashraf: Data curation, Formal analysis, and . **Gustavo M. Castelluccio:** Conceptualization, Methodology, development, Funding acquisition, and manuscript preparation.

Declaration of competing interest

The authors declare that they have no known competing financial interests or personal relationships that could have appeared to influence the work reported in this paper.

Acknowledgment

The first author is grateful for the support of The Punjab Educational Endowment Fund (PEEF) for funding the project. The corresponding author thanks The Engineering and Physical Sciences Research Council (UK) for funding under EPSRC grant EP/R034478/1.

Appendix A. Supplementary data

Supplementary data to this article can be found online at https://doi.org/10.1016/j.msea.2022.142972.

References

[1] P. Li, S.X. Li, Z.G. Wang, Z.F. Zhang, Fundamental factors on formation mechanism of dislocation arrangements in cyclically deformed fcc single crystals, Prog. Mater. Sci. 56 (2011) 328–377, https://doi.org/10.1016/j.pmatsci.2010.12.001.
[2] A. Oudriss, X. Feaugas, Length scales and scaling laws for dislocation cells developed during monotonic deformation of (001) nickel single crystal, Int. J. Plast. 78 (2016) 187–202, https://doi.org/10.1016/j.ijplas.2015.11.003.
[3] H. Nahm, J. Moteff, D.R. Diercks, Substructural development during low cycle fatigue of AISI 304 stainless steel at 649°C, Acta Metall. 25 (1977) 107–116, https://doi.org/10.1016/0001-6160(77)90114-6.
[4] Y. Estrin, L.S. Tóth, A. Molinari, Y. Bréchet, A dislocation-based model for all hardening stages in large strain deformation, Acta Mater. 46 (1998) 5509–5522, https://doi.org/10.1016/S1359-6454(98)00196-7.
[5] L.S. Tóth, A. Molinari, Y. Estrin, Strain hardening at large strains as predicted by dislocation based polycrystal plasticity model, Journal of Engineering Materials and Technology, Transactions of the ASME 124 (2002) 71–77, https://doi.org/10.1115/1.1421350.
[6] M. Berveiller, A. Zaoui, Some applications of the self-consistent scheme in the field of plasticity and texture of metallic polycrystals, in: J. Gittus, J. Zarka, S. Nemat-Nasser (Eds.), Large Deformations of Solids: Physical Basis and Mathematical Modelling, Springer Netherlands, 1986, pp. 223–241, https://doi.org/10.1007/978-94-009-3407-8_14.
[7] J. Fajoui, D. Gloaguen, B. Courant, R. Guillén, Micromechanical modelling of the elastoplastic behaviour of metallic material under strain-path changes, Comput. Mech. 44 (2009) 285–296, https://doi.org/10.1007/s00466-009-0374-7.
[8] G.M. Castelluccio, D.L. McDowell, Mesoscale cyclic crystal plasticity with dislocation substructures, Int. J. Plast. 98 (2017) 1–26, https://doi.org/10.1016/j.ijplas.2017.06.002.
[9] R. Mura, T.C.T. Ting, Micromechanics of defects in solids, J. Appl. Mech. 56 (1989) 487–488, https://doi.org/10.1115/1.3176116, 2nd rev.
[10] S. Dindarlou, G.M. Castelluccio, Substructure-sensitive crystal plasticity with material-invariant parameters, Int. J. Plast.. Under review (n.d.).
[11] A.M. Hussein, S.I. Rao, M.D. Uchic, D.M. Dimiduk, J.A. El-Awady, Microstructurally based cross-slip mechanisms and their effects on dislocation microstructure evolution in fcc crystals, Acta Mater. 85 (2015) 180–190, https://doi.org/10.1016/j.actamat.2014.10.067.
[12] S. Xia, A. El-Azab, Computational modelling of mesoscale dislocation patterning and plastic deformation of single crystals, Model. Simulat. Mater. Sci. Eng. 23 (2015), 055009, https://doi.org/10.1088/0965-0393/23/5/055009.
[13] R. Wu, M. Zaiser, Cell structure formation in a two-dimensional density-based dislocation dynamics model, Mater Theory 5 (2021) 3, https://doi.org/10.1186/s41313-020-00025-x.
[14] M. Sauzay, L.P. Kubin, Scaling laws for dislocation microstructures in monotonic and cyclic deformation of fcc metals, Prog. Mater. Sci. 56 (2011) 725–784, https://doi.org/10.1016/j.pmatsci.2011.01.006.
[15] L. Kubin, M. Sauzay, Persistent slip bands: similitude and its consequences, Acta Mater. 104 (2016) 295–302, https://doi.org/10.1016/j.actamat.2015.11.010.
[16] L. Kubin, M. Sauzay, Persistent slip bands: the bowing and passing model revisited, Acta Mater. 132 (2017) 517–524, https://doi.org/10.1016/j.actamat.2017.04.064.
[17] P. Li, S.X. Li, Z.G. Wang, Z.F. Zhang, Fundamental factors on formation mechanism of dislocation arrangements in cyclically deformed fcc single crystals, Prog. Mater. Sci. 56 (2011) 328–377, https://doi.org/10.1016/j.pmatsci.2010.12.001.
[18] M. Videm, N. Ryum, Cyclic deformation of [001] aluminium single crystals, Mater. Sci. Eng. 219 (1996) 1–10, https://doi.org/10.1016/S0921-5093(96)10261-6.
[19] J. Bretschneider, C. Holste, B. Tippelt, Cyclic plasticity of nickel single crystals at elevated temperatures, Acta Mater. 45 (1997) 3775–3783, https://doi.org/10.1016/S1359-6454(97)00030-X.
[20] Z.S. Basinski, S.J. Basinski, Fundamental aspects of low amplitude cyclic deformation in face-centred cubic crystals, Prog. Mater. Sci. 36 (1992) 89–148, https://doi.org/10.1016/0079-6425(92)90006-S.
[21] J.M. Finney, C. Laird, Strain localization in cyclic deformation of copper single crystals, Phil. Mag. 31 (1975) 339–366, https://doi.org/10.1080/14786437508228937.
[22] J. Yang, Y. Li, S. Li, C. Ma, G. Li, Simulation and observation of dislocation pattern evolution in the early stages of fatigue in a copper single crystal, Mater. Sci. Eng. 299 (2001) 51–58, https://doi.org/10.1016/S0921-5093(00)01415-5.
[23] L. Buchinger, S. Stanzl, C. Laird, Dislocation structures in copper single crystals fatigued at low amplitudes, Philos. Mag. A: Physics of Condensed Matter, Structure, Defects and Mechanical Properties 50 (1985) 275–298, https://doi.org/10.1080/01418618408244227.
[24] J.C. Grosskreutz, The mechanisms of metal fatigue (I), Phys. Status Solidi 47 (1971) 11–31, https://doi.org/10.1002/pssb.2220470102.
[25] S.E. Stanzl-Tschegg, B. Schönbauer, Mechanisms of strain localization, crack initiation and fracture of polycrystalline copper in the VHCF regime, Int. J. Fatig. 32 (2010) 886–893, https://doi.org/10.1016/j.ijfatigue.2009.03.016.
[26] C. Holste, Cyclic plasticity of nickel, from single crystals to submicrocrystalline polycrystals, Phil. Mag. 84 (2004) 299–315, https://doi.org/10.1080/14786430310001610357.
[27] L. Buchinger, S. Stanzl, C. Laird, C. Laird, Dislocation structures produced by low-amplitude fatigue of copper single crystals at 77 K, Philos. Mag. A: Physics of Condensed Matter, Structure, Defects and Mechanical Properties 62 (1990) 633–651, https://doi.org/10.1080/01418619008244797.
[28] P. Charsley, L.J. Harris, Condensed dislocation structures in polycrystalline aluminium fatigued at 77K, Scripta Metall. 21 (1987) 341–344, https://doi.org/10.1016/0036-9748(87)90225-0.
[29] M.E. Kassner, M.A. Wall, M.A. Delos-Reyes, Microstructure and mechanisms of cyclic deformation of aluminum single crystals at 77 K, Metall. Mater. Trans.: Physical Metallurgy and Materials Science 28 (1997) 595–609, https://doi.org/10.1007/s11661-997-0045-2. A.
[30] D.J. Morrison, V. Chopra, Cyclic stress-strain response of polycrystalline nickel, Mater. Sci. Eng. 177 (1994) 29–42, https://doi.org/10.1016/0921-5093(94)90475-8.
[31] Y. El-Madhoun, A. Mohamed, M.N. Bassim, Cyclic stress-strain behavior of polycrystalline nickel, Mater. Sci. Eng. 385 (2004) 140–147, https://doi.org/10.1016/j.msea.2004.06.064.
[32] Z.S. Basinski, A.S. Korbel, S.J. Basinski, The temperature dependence of the saturation stress and dislocation substructure in fatigued copper single crystals, Acta Metall. 28 (1980) 191–207, https://doi.org/10.1016/0001-6160(80)90068-1.
[33] U. Essmann, H. Mughrabi, Annihilation of dislocations during tensile and cyclic deformation and limits of dislocation densities, Philos. Mag. A: Physics of Condensed Matter, Structure, Defects and Mechanical Properties 40 (1979) 731–756, https://doi.org/10.1080/01418617908234871.
[34] M. Gerland, J. Mendez, P. Violan, B. Ait Saadi, Evolution of dislocation structures and cyclic behaviour of a 316L-type austenitic stainless steel cycled in vacuo at room temperature, Mater. Sci. Eng. 118 (1989) 83–95, https://doi.org/10.1016/0921-5093(89)90060-9.
[35] H. Mughrabi, The cyclic hardening and saturation behaviour of copper single crystals, Mater. Sci. Eng. 33 (1978) 207–223, https://doi.org/10.1016/0025-5416(78)90174-X.
[36] U. Holzwarth, U. Essmann, Temperature-induced rearrangement of the dislocation pattern of Persistent Slip Bands in copper single crystals, Applied Physics A Solids and Surfaces 58 (1994) 197–210, https://doi.org/10.1007/BF00324376.
[37] Y. Nakanishi, H. Tanaka, T. Fujii, S. Onaka, M. Kato, Low-temperature fatigue behaviour and development of dislocation structure in aluminium single crystals

with single-slip orientation, Phil. Mag. 93 (2013) 2759–2768, https://doi.org/10.1080/14786435.2013.786193.
[38] P. Hähner, B. Tippelt, C. Holste, On the dislocation dynamics of persistent slip bands in cyclically deformed F.C.C. metals, Acta Mater. 46 (1998) 5073–5084, https://doi.org/10.1016/S1359-6454(98)00161-X.
[39] B. Tippelt, J. Bretschneider, P. Hähner, The dislocation microstructure of cyclically deformed nickel single crystals at different temperatures, Physica Status Solidi (A) Applied Research 163 (1997) 11–26, https://doi.org/10.1002/1521-396X(199709)163:1<11:AID-PSSA11>3.0.CO;2-X.
[40] D.J. Morrison, V. Chopra, Cyclic stress-strain response of polycrystalline nickel 177 (1994) 29–42.
[41] Z.S. Basinski, A.S. Korbel, S.J. Basinski, The temperature dependence of the saturation stress and dislocation substructure in fatigued copper single crystals, Acta Metall. 28 (1980) 191–207, https://doi.org/10.1016/0001-6160(80)90068-1.
[42] H. Shirai, J.R. Weertman, Fatigue dislocation structures at elevated temperatures, Scripta Metall. 17 (1983) 1253–1258, https://doi.org/10.1016/0036-9748(83)90294-6.
[43] L.L. Lisiecki, J.R. Weertman, Orientation effects on the elevated temperature fatigue of copper single crystals, Acta Metall. Mater. 38 (1990) 509–519, https://doi.org/10.1016/0956-7151(90)90157-C.
[44] P. Li, Z.F. Zhang, S.X. Li, Z.G. Wang, Cyclic deformation and fatigue damage behaviors of [image omitted] oriented Ag single crystal, Phil. Mag. 89 (2009) 2903–2920, https://doi.org/10.1080/14786430903130847.
[45] P. Li, S.X. Li, Z.G. Wang, Z.F. Zhang, Dislocation arrangements in cyclically deformed Au single crystal, Mater. Sci. Eng. 527 (2010) 6244–6247, https://doi.org/10.1016/j.msea.2010.06.040.
[46] M.S. Pham, S.R. Holdsworth, K.G.F. Janssens, E. Mazza, Cyclic deformation response of AISI 316L at room temperature: mechanical behaviour, microstructural evolution, physically-based evolutionary constitutive modelling, Int. J. Plast. 47 (2013) 143–164, https://doi.org/10.1016/j.ijplas.2013.01.017.
[47] F. Boehme, K. Hidaka, J.R. Weertman, PSB observation in copper fatigued at one half the melting temperature, Scripta Metall. Mater. 24 (1990) 2341–2346, https://doi.org/10.1016/0956-716X(90)90090-4.
[48] J. Polák, V. Mazánová, M. Heczko, I. Kuběna, J. Man, Profiles of persistent slip markings and internal structure of underlying persistent slip bands, Fatig. Fract. Eng. Mater. Struct. 40 (2017) 1101–1116, https://doi.org/10.1111/ffe.12567.
[49] P. Spätig, M. Heczko, T. Kruml, H.P. Seifert, Influence of mean stress and light water reactor environment on fatigue life and dislocation microstructures of 316L austenitic steel, J. Nucl. Mater. 509 (2018) 15–28, https://doi.org/10.1016/j.jnucmat.2018.05.064.
[50] A.T. Winter, O.R. Pedersen, K.V. Rasmussen, Dislocation microstructures in fatigued copper polycrystals, Acta Metall. 29 (1981) 735–748, https://doi.org/10.1016/0001-6160(81)90117-6.
[51] L. Boulanger, A. Bisson, A.A. Tavassoli, Labyrinth structure and persistent slip bands in fatigued 316 stainless steel, Philos. Mag. A: Physics of Condensed Matter, Structure, Defects and Mechanical Properties 51 (1985), https://doi.org/10.1080/01418610.1985.12069154. L5–L11.
[52] T. Fujii, T. Kajita, T. Miyazawa, S. Arai, Characterization of dislocation microstructures in cyclically deformed [001] copper single crystals using high voltage scanning transmission electron microscopy, Mater. Char. 136 (2018) 206–211, https://doi.org/10.1016/j.matchar.2017.12.026.
[53] C. Laird, P. Charsley, H. Mughrabi, Low energy dislocation structures produced by cyclic deformation, Mater. Sci. Eng. 81 (1986) 433–450, https://doi.org/10.1016/0025-5416(86)90281-8.
[54] S.E. Fielding, W.M. Stobbs, Dislocation structures in fatigued polycrystalline stainless steel, J. Microsc. 130 (1983) 279–288, https://doi.org/10.1111/j.1365-2818.1983.tb04548.x.
[55] N.Y. Jin, A.T. Winter, Dislocation structures in cyclically deformed [001] copper crystals, Acta Metall. 32 (1984) 1173–1176, https://doi.org/10.1016/0001-6160(84)90123-8.
[56] P.J. Jackson, D. Kuhlmann-Wilsdorf, Low-energy dislocation cell structures produced by cross-slip, Scripta Metall. 16 (1982) 105–107, https://doi.org/10.1016/0036-9748(82)90412-4.
[57] Y. El-Madhoun, A. Mohamed, M.N. Bassim, Cyclic stress-strain response and dislocation structures in polycrystalline aluminum, Mater. Sci. Eng. 359 (2003) 220–227, https://doi.org/10.1016/S0921-5093(03)00347-2.
[58] C.E. Feltner, Dislocation arrangements in aluminum deformed by repeated tensile stresses, Acta Metall. 11 (1963) 817–828, https://doi.org/10.1016/0001-6160(63)90021-X.
[59] C.E. Feltner, Dislocation debris in aluminium fatigued at 78°K, Phil. Mag. 8 (1963) 2121–2124, https://doi.org/10.1080/14786436308209107.
[60] S.P. Bhat, C. Laird, High temperature cyclic deformation OF nickel, Fatig. Fract. Eng. Mater. Struct. 1 (1979) 59–77, https://doi.org/10.1111/j.1460-2695.1979.tb00367.x.
[61] E.S. Kayali, A. Plumtree, Stress-substructure relationships in cyclically and monotonically deformed wavy slip mode metals, Metall. Trans. A 13 (1982) 1033–1041, https://doi.org/10.1007/BF02643400.
[62] J.C. Grosskreutz, Development of substructure in polycrystalline aluminum during constant-strain fatigue, J. Appl. Phys. 34 (1963) 372–379.
[63] M.R. Staker, D.L. Holt, The dislocation cell size and dislocation density in copper deformed at temperatures between 25 and 700°C, Acta Metall. 20 (1972) 569–579, https://doi.org/10.1016/0001-6160(72)90012-0.
[64] J.E. Pratt, Dislocation substructure in strain-cycled copper as influenced by temperature, Acta Metall. 15 (1967) 319–327, https://doi.org/10.1016/0001-6160(67)90208-8.
[65] P. Ambrosi, E. Göttler, C. Schwink, On the dislocation arrangement and flow stress of [111] - copper single crystals deformed in tension, Scripta Metall. 8 (1974) 1093–1097, https://doi.org/10.1016/S0036-9748(74)80010-4.
[66] D. Knoesen, S. Kritzinger, Dislocation cell boundary widths and dislocation cell sizes in deformed copper, Acta Metall. 30 (1982) 1219–1222, https://doi.org/10.1016/0001-6160(82)90017-7.
[67] S. El Shawish, L. Cizelj, Combining single- and poly-crystalline measurements for identification of crystal plasticity parameters: application to austenitic stainless steel, Crystals 7 (2017) 181, https://doi.org/10.3390/cryst7060181.
[68] H. Pirgazi, L.A.I. Kestens, Semi in-situ observation of crystal rotation during cold rolling of commercially pure aluminum, Mater. Char. 171 (2021) 110752, https://doi.org/10.1016/j.matchar.2020.110752.
[69] F. Ashraf, G.M. Castelluccio, A robust approach to parameterize dislocation glide energy barriers in FCC metals and alloys, J. Mater. Sci. 56 (2021) 16491–16509, https://doi.org/10.1007/s10853-021-06376-1.
[70] K. Sedighiani, M. Diehl, K. Traka, F. Roters, J. Sietsma, D. Raabe, An efficient and robust approach to determine material parameters of crystal plasticity constitutive laws from macro-scale stress–strain curves, Int. J. Plast. 134 (2020) 102779, https://doi.org/10.1016/j.ijplas.2020.102779.
[71] K. Sedighiani, K. Traka, F. Roters, D. Raabe, J. Sietsma, M. Diehl, Determination and analysis of the constitutive parameters of temperature-dependent dislocation-density-based crystal plasticity models, Mech. Mater. 164 (2022) 104117, https://doi.org/10.1016/j.mechmat.2021.104117.
[72] G.M. Castelluccio, H. Lim, J.M. Emery, C.C. Battaile, Crack tip microplasticity mediated by microstructure gradients, Fatig. Fract. Eng. Mater. Struct. 44 (2021) 2337–2355, https://doi.org/10.1111/ffe.13493.
[73] H.M. Ma, X.-L. Gao, Strain gradient solution for a finite-domain Eshelby-type plane strain inclusion problem and Eshelby's tensor for a cylindrical inclusion in a finite elastic matrix, Int. J. Solid Struct. 48 (2011) 44–55, https://doi.org/10.1016/j.ijsolstr.2010.09.004.
[74] Kakandar, Ebiakpo, Alejandro Barrios, Johann Michler, Xavier Maeder, Olivier N. Pierron, and Gustavo M. Castelluccio. A Computational and Experimental Comparison on the Nucleation of Fatigue Cracks in Statistical Volume Elements. Int. J. Fatig., 137 (1 August 2020): 105633. doi: 10.1016/j.ijfatigue.2020.105633.

https://dspace.org/

On the similitude relation for dislocation wall thickness under cyclic deformation

Ashraf, Farhan; Castelluccio, Gustavo M.

2022-03-10
Elsevier
https://doi.org/10.1016/j.msea.2022.142972
Ashraf F, Castelluccio G. (2022) On the similitude relation for dislocation wall thickness under cyclic deformation, Materials Science and Engineering A: Structural Materials: Properties, Microstructures and Processing, Volume 840, April 2022, Article number 142972

Downloaded from a DSpace repository. https://dspace.org/